Kinetics of Normal Grain Growth Depending on the Size Distribution of Small Grains

Article *in* MATERIALS TRANSACTIONS · October 2004

DOI: 10.2320/jinstmet.68.913

3 authors, including:

Byung-Nam Kim
National Institute for Materials Science
224 PUBLICATIONS **3,578** CITATIONS

SEE PROFILE

Keijiro Hiraga
National Institute for Materials Science
191 PUBLICATIONS **3,465** CITATIONS

SEE PROFILE

Materials Transactions, Vol. 44, No. 11 (2003) pp. 2239 to 2244

Kinetics of Normal Grain Growth Depending on the Size Distribution of Small Grains

Byung-Nam Kim*, Keijiro Hiraga and Koji Morita

Center for Structural Materials Research, National Institute for Materials Science, Tsukuba 305-0047, Japan

A theoretical relationship is derived between the kinetics of normal grain growth and the size distribution of small grains. When the distribution of the normalized grain size r is proportional to r^m around $r = 0$ in a steady state, the grain growth exponent n is revealed to be $m + 1$. The same relationship is also derived from the analysis of the mean field model for particle growth. The validity of this relationship is confirmed from the consistence with existing grain-growth models and numerical simulations. Experimental consistence is observed for the size distribution on sectional surface. It is found that a log-normal function is not a steady-state size distribution for normal grain growth with $n = 2$, even though it may approximate experimental size distributions. The obtained relationship is also shown to be applicable to particle coarsening by Ostwald-ripening.

(Received June 20, 2003; Accepted September 1, 2003)

Keywords: *grain growth, grain annihilation, size distribution, steady state, particle coarsening*

1. Introduction

Normal grain growth is defined as the uniform increase in the average grain size of a polycrystalline aggregate, due to the annihilation of small grains by grain boundary migration. The kinetics of normal grain growth is generally represented by

$$\langle R\rangle^n - \langle R\rangle_0^n = kt \tag{1}$$

where t is the time, $\langle R\rangle$ is the average grain radius at t, $\langle R\rangle_0$ is the initial value of $\langle R\rangle$ at $t = 0$, n is the grain growth exponent and k is the kinetic coefficient. On normal grain growth, there have been extensive studies including the curvature-driven growth model,[1] diffusion-like growth model,[2] statistical analysis,[3] stochastic model[4] and numerical simulations.[5–12] Despite a variety of the analyzing methods, most of the studies predict an n-value of 2, and thereby $n = 2$ has widely been recognized as the theoretical grain growth exponent for normal grain growth.

In those studies giving $n = 2$, however, the obtained size distributions of grains in a steady state are various. Some models assert a log-normal function,[5,13,14] and others different functions.[1,2] Despite the variety of the size distributions, the same n-value of 2 has been derived. In particular, a log-normal distribution of grain size has also been reported for some actual materials with $n \neq 2$.[15] It thus appears that there is no tight relationship between the grain growth exponent and the size distribution. Then, what is the effect of the size distribution on the grain growth kinetics? In the present study, we examine the theoretical relationship between the grain growth kinetics and the size distribution in a steady state. We show that the size distribution of small grains is directly related to the grain growth exponent, and that the relationship is available in both ideal and actual materials. We also show that the present analysis is applicable to particle coarsening by Ostwald-ripening.

*Corresponding author, E-mail: kim.byung-nam@nims.go.jp

2. Growth Kinetics by Grain Annihilation

Normal grain growth occurs eventually through the annihilation of small grains with 4-faces in a 3-dimensional (3D) polycrystalline structure. In the growth process, the number of faces for grains smaller than a critical grain size decreases gradually to 4, and finally to 0, namely, grain annihilation. The minimum number of faces available for 3D grains is 4. Although some grains can have 2- or 3-faces when they locate at grain boundaries or triple junctions, the probability seems to be extremely low so that the effect on the grain growth kinetics is negligible. Almost all of the grains with extremely small sizes are tetrahedra prior to annihilation.

According to the von Neumann-Mullins law,[16] when a grain boundary migrates with a driving force originating from its curvature, the growth rate dR^2/dt of grains with radius R in a 2-dimensional (2D) polycrystalline structure depends solely on the number of the grain edges. Mullins[17] later extended the law to 3D, and derived an equivalent relation between the growth rate and the number of faces. Although the relation varies depending on the shape of the component polygonal faces, it holds for the mean value of grains with the same number of faces and was verified by a 3D simulation of grain growth.[12] Accordingly, for such ideal polycrystalline materials, the growth rate dR^2/dt can be regarded as a constant for tetrahedra, independently of their sizes. Then, the grain radius R_h, below which tetrahedra disappear during an infinitesimal time of Δt, is obtained as ${R_h}^2 = c\Delta t$, where c is a constant. For both nano-grained and coarse-grained materials, the value of R_h is the same and dependent only on Δt, if the von Neumann-Mullins law holds.

The same concept can be applied to actual polycrystalline materials, where the driving force for grain boundary migration is generally unequal to the curvature of grain boundary. In actual polycrystalline materials, grain boundary migration is often controlled by solute-drag or by particle-pinning. Even in these cases, however, normal grain growth occurs by the same way, namely, by the annihilation of small

grains. Independently of the mechanism of grain boundary migration, there will exist the grain radius R_h below which tetrahedra disappear during Δt in a steady state, and the disappearance of the tetrahedra smaller than R_h causes eventually grain growth. The only difference from the above ideal case is the relationship between R_h and Δt.

The number of grains disappearing during Δt can be calculated from the size distribution. Here, we represent the normalized size distribution $F(r)$ as ar^m around $r = 0$, where $F(r)$ is the probability density function, r is $R/\langle R\rangle$, and a and m are constants. As will be shown later, this function corresponds to a solution of the size distribution around $r = 0$ in the mean field model, when the growth kinetics is represented by eq. (1). Since the grain size distribution $F(r)$ is self-similar in a steady state, the normalized distribution holds the same form throughout the grain growth process. By supposing a steady-state grain growth, we cut down the detailed topological changes due to the grain annihilation. Then, the number of tetrahedra ΔN disappearing during Δt is calculated by

$$\Delta N = -\beta N \int_0^{r_h} ar^m \mathrm{d}r = -\frac{a\beta N}{m+1} {r_h}^{m+1} \tag{2}$$

where N is the total number of grains, and β is the ratio of the number of grains with 4-faces to the number of all grains for $R \leq R_h$. In a steady state, β is constant, if the size distributions for all classes of grains with more than 4-faces are represented as the same form ar^m around $r = 0$. Comparing ΔN with that at the initial stage ΔN_0, we obtain

$$\frac{\Delta N}{\Delta N_0} = \frac{N}{N_0}\left(\frac{R_h/\langle R\rangle}{R_h/\langle R\rangle_0}\right)^{m+1} = \frac{N}{N_0}\left(\frac{\langle R\rangle_0}{\langle R\rangle}\right)^{m+1}. \tag{3}$$

For the average grain radius $\langle R\rangle$, we define

$$\langle R\rangle^3 = 3V_T/(4\pi N) \tag{4}$$

where V_T is the total grain volume. For self-similar grain growth in three dimensions, conservation of the total grain volume gives a relationship of

$$N/N_0 = (\langle R\rangle_0/\langle R\rangle)^3 \tag{5}$$

and then, eq. (3) can be rewritten as

$$\Delta N/\Delta N_0 = (\langle R\rangle_0/\langle R\rangle)^{m+4}. \tag{6}$$

Another relationship between ΔN and $\langle R\rangle$ can be derived by differentiating eq. (4) and using eq. (5):

$$\frac{\Delta N}{\Delta N_0} = \left(\frac{\langle R\rangle_0}{\langle R\rangle}\right)^4 \frac{\Delta\langle R\rangle}{\Delta\langle R\rangle_0} \tag{7}$$

From eqs. (6) and (7), the ratio of the increment in the average grain radius at an arbitrary stage $\Delta\langle R\rangle$ to that at the initial stage $\Delta\langle R\rangle_0$ is obtained as

$$\Delta\langle R\rangle/\Delta\langle R\rangle_0 = (\langle R\rangle_0/\langle R\rangle)^m. \tag{8}$$

Equation (8) is a general representation for the kinetics of normal grain growth relating to the grain-size distribution, independently of the mechanism of grain boundary migration. The relationship identical to eq. (8) is also obtained in two dimensions. Equation (8) can be compared with the differentiation of eq. (1):

$$\Delta\langle R\rangle/\Delta\langle R\rangle_0 = (\langle R\rangle_0/\langle R\rangle)^{n-1}. \tag{9}$$

Then, from eqs. (8) and (9), we consequently obtain

$$n = m + 1. \tag{10}$$

This relationship between n and m depends on the function $F(r)$ defined around $r = 0$, and hence different $F(r)$ results in a different n-m relationship. Of the size distribution functions available to the present analysis, however, $F(r) = ar^m$ around $r = 0$ has a merit of simplicity and independency of the mechanism of grain-boundary migration. In the following, we give a physical basis to this function, by showing that eq. (10) can also be derived from the mean field model for growth kinetics of particles.

3. Mean Field Model

For describing the growth kinetics of grains, Hillert[1)] adapted the classical mean field model for particle coarsening. According to the model, the growth law of an individual grain or particle can be represented in a generalized form as

$$G = \frac{\mathrm{d}R}{\mathrm{d}t} = \frac{K}{R^{n-1}}\left(\frac{R}{R_c} - 1\right) = \frac{K}{R^{n-1}}(r_c - 1) \tag{11}$$

where K is a constant, R_c is the critical radius, and r_c is R/R_c. In eq. (11), the value of n is 2 and 3 for normal grain growth and particle coarsening by Ostwald-ripening, respectively. For grain growth in actual materials, the value of n in eq. (1) is generally larger than 2. Even in these cases, however, we consider that the equivalent mean field description can be given by eq. (11). In other words, we consider that n can have an arbitrary value larger than 2, depending on the growth mechanism. Using eq. (11), $\mathrm{d}r_c/\mathrm{d}t(= G^*)$ can be written as

$$G^* = \frac{\mathrm{d}r_c}{\mathrm{d}t} = \frac{1}{R_c}\frac{\mathrm{d}R_c}{\mathrm{d}t} g(r_c) \tag{12}$$

where

$$g(r_c) = \frac{1}{r_c^{n-1}}[v(r_c - 1) - r_c^n] \tag{13}$$

and

$$v = K\left[R_c^{n-1}\frac{\mathrm{d}R_c}{\mathrm{d}t}\right]^{-1} = nK\left[\frac{\mathrm{d}R_c^n}{\mathrm{d}t}\right]^{-1} = nK\gamma^n\left[\frac{\mathrm{d}\langle R\rangle^n}{\mathrm{d}t}\right]^{-1}. \tag{14}$$

Although the value of the ratio $\langle R\rangle/R_c$ $(= \gamma = r_c/r)$ depends on the size distribution, it is constant in a steady state. Thus, the value of v should be constant, in order for the growth kinetics of the mean field model to be represented by eq. (1).

Using the analysis by Coughlan and Fortes,[18)] the fraction of the number of grains disappearing during $\mathrm{d}t$ is obtained as

$$\frac{1}{N}\frac{\mathrm{d}N}{\mathrm{d}t} = \left[H(r_c)G^*\right]_{r_c=0} = \frac{v}{R_c}\frac{\mathrm{d}R_c}{\mathrm{d}t}\left[H(r_c)\left(\frac{1}{r_c^{n-2}} - \frac{1}{r_c^{n-1}}\right)\right]_{r_c=0} \tag{15}$$

where $H(r_c)$ is the probability density function with respect to r_c. From this equation and the differentiation of eq. (4), we obtain

$$H(r_c) \approx \frac{\alpha}{v} r_c^{n-1} \quad \text{around} \quad r_c = 0 \tag{16}$$

where $\alpha = 2$ in two dimensions and $\alpha = 3$ in three dimensions. Since $F(r) = \gamma H(r_c)$ and $r_c = \gamma r$, eq. (16) is the same form with $F(r) = ar^{n-1}$ shown in the previous section. The full description of $H(r_c)$ for the whole range of r_c was carried out by Hillert[1] and Rios[19] for normal grain growth ($n = 2$), and by Brown[20] and Coughlan and Fortes[18] for particle coarsening by Ostwald-ripening ($n = 3$).

The mean field model is insufficient to describe detailed grain growth behavior. For example, 2D grains smaller than R_c do shrink independently of the number of edges, which is contradictory to the von Neumann-Mullins law.[16] The mean field model, however, has widely been recognized to describe the general features of normal grain growth, including growth kinetics and size distribution. Hence, we consider that eq. (16) derived from the mean field model can provide the physical basis of the size distribution $F(r) = ar^m$ employed in the previous section.

4. Comparison with Other Models and Experiments

4.1 Theoretical models

For parabolic grain growth ($n = 2$), eq. (10) predicts $m = 1$, that is, the size distribution around $r = 0$ is linear with respect to the grain size. The linear dependence is observed in theoretical size distributions. The following is the theoretical representative of the size distribution for normal grain growth with $n = 2$: Hillert's function and Rayleigh function. Hillert[1] derived an expression for the size distribution from the mean field model of eq. (11), for the special case of $v = 4$ in eq. (14). In his model, there is only one asymptotic steady-state size distribution. The Hillert's function $H(r_c)$ in three dimensions is represented as

$$H(r_c) = (2e)^3 \frac{3r_c}{(2 - r_c)^5} \exp\left[\frac{-6}{2 - r_c}\right]. \tag{17}$$

Rayleigh function[2] as a steady-state size distribution of grains was derived from the diffusion-like grain growth model where grains grow or shrink by random walk in the grain size-time space. Although the physical basis of the model is ambiguous, the obtained size distribution shows good consistence with some numerical simulations.[10,11] The Rayleigh function $H(r_c)$ is represented as[21]

$$H(r_c) = 3r_c \exp\left[\frac{-3}{2} r_c^2\right]. \tag{18}$$

In eqs. (17) and (18), r_c can be replaced with r, using $\gamma = r_c/r = \langle R\rangle/R_c$. From the definition of $\langle R\rangle$ in eq. (4), $\langle R\rangle^3$ is equal to $\overline{R^3}$ $(= \int R^3 F(r)\mathrm{d}r = \int R^3 H(r_c)\mathrm{d}r_c)$, so that the value of γ is obtained from the relationship $\gamma^3 = \langle R\rangle^3/{R_c}^3 = \overline{R^3}/{R_c}^3 = \overline{{r_c}^3}$, where

$$\overline{r_c^3} = \int_0^\infty r_c^3 H(r_c)\mathrm{d}r_c. \tag{19}$$

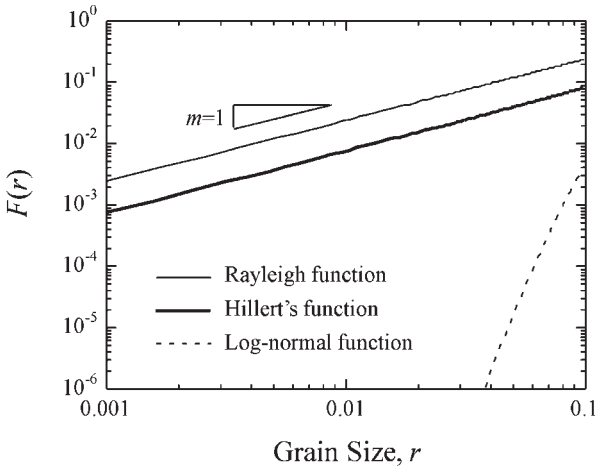

Fig. 1 Theoretical and log-normal ($\sigma = 0.5$) size distributions of grains.

Calculating numerically eq. (19) with eq. (17) or eq. (18), we obtain the γ-value of 0.985 or 0.898, respectively. Then, we can represent the size distribution $F(r)$ in the Hillert's and Rayleigh functions, by replacing $H(r_c)$ and r_c with $F(r)/\gamma$ and γr, respectively.

As illustrated in Fig. 1, the Hillert's and Rayleigh functions that give $n = 2$ follow the size distribution of $m = 1$ around $r = 0$, supporting the validity of eq. (10). As apparent in the above analysis, $3\gamma^2 r/4$ ($\gamma = 0.985$) and $3\gamma^2 r$ ($\gamma = 0.898$) are also obtained as a first-order approximation around $r = 0$ in three dimensions for the Hillert's and Rayleigh functions, respectively. In other words, the two functions satisfy the condition of $m = 1$, which is necessary for retaining the steady-state size distribution with $n = 2$. According to the mean field analyses, it is known that there are an infinite number of possible size distributions with different v-values in a steady state of grain growth[19] and of particle coarsening.[18,20] We consider that the situation is similar to the different models on normal grain growth, because the Hillert's and Rayleigh functions, as well as the numerical simulations that will appear in Section 4.3, show various steady-state size distributions for the same growth kinetics ($n = 2$). In addition to the size distributions predicted by the mean field model, there will also be an infinite number of possible steady-state size distributions for grain growth with a given n-value. Hence, in determining and evaluating the size distribution functions, eq. (10) can provide one of the criteria that should be satisfied in a steady state.

4.2 Log-normal function

Despite a lack of physical basis, a log-normal function has widely been used to describe experimentally-observed size distributions.[13–15,22–24] The log-normal function as the steady-state size distribution can be represented as

$$F(r) = \frac{1}{(2\pi\sigma^2)^{1/2} r} \exp\left[-\frac{(\ln\gamma - \ln r_m)^2}{2\sigma^2}\right] \tag{20}$$

where σ is the standard deviation and r_m is the median of the distribution. Takayama *et al.*[25] calculated the value of r_m in this equation to be $\exp(-3\sigma^2/2)$, for an array of tetrakaidecahedra.

The log-normal function, however, shows nonlinear

dependence around $r = 0$: the m-value increases steeply with decreasing r, as illustrated in Fig. 1. Thus, the present analysis implies that the log-normal function does not represent the size distribution for normal grain growth with $n = 2$. In order for this function to be a steady-state size distribution, the value of n should considerably be larger than 2. This situation may arise from the lack of physical basis. Although Kurtz and Carpay[14] tried to derive the physical origin of the log-normal function for normal grain growth, Atkinson[26] pointed out a critical mistake in their model. At present, "the general applicability of the log-normal distribution to grain growth is not universally accepted", as Atkinson[26] concluded.

For the log-normal distribution, we should note the following critical point. If a log-normal function is the size distribution in a steady state, the corresponding grain growth exponent n should be fixed. Although a fixed n-value allows various size distributions, as mentioned in the previous section, the reverse case is not allowed. However, just the unallowable case has been the experimental size distributions fitted to the log-normal function, in materials with different n-values.[13–15,22–24] Hence, to rationalize the log-normal function as a steady-state size distribution, it should not be derived from empirical curve fitting, but from theoretical analysis of normal grain growth.

4.3 Numerical simulations

Many numerical simulations on normal grain growth have yielded parabolic grain growth ($n = 2$) and linear distribution of grain size around $r = 0$. The linear distribution is illustrated in Fig. 2, where the size distributions $F(r)$ in the following simulations depend linearly on r for small grain sizes: the vertex model,[6,10] 2D Monte Carlo model,[7] variational principle,[8] Surface Evolver program[9] and atomic jump model,[11] where $n = 2$ has been obtained. A slightly increasing m-value with decreasing r in the 3D vertex model[6] may occur from insufficient data for such small grains.

The exception of the linear dependence appears for the 3D Monte Carlo simulation,[5] for which the size distribution is characterized with $m = 2.0 \sim 3.0$ for small grains, as shown in Fig. 2. This m-value predicts $n = 3.0 \sim 4.0$ from eq. (10),

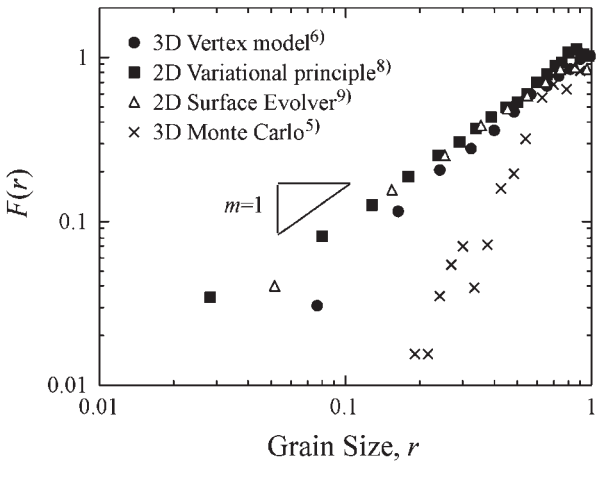

Fig. 2 Simulated size distributions of small grains.

and the prediction is consistent with $n = 2.6 \sim 3.6$ obtained in the 3D Monte Carlo simulation.[5] Hence, we can conclude that eq. (10) is valid for representing the relationship between the grain growth kinetics and the size distribution of small grains.

Here, we should discuss the valid range of $F(r) = ar^m$ in comparing with measured size distributions. In a strict sense, the valid range must be extremely small around $r = 0$, but it can be extended by using a first-order approximation. Let us consider a 2D case. In a steady state, it is known that the size distributions of all classes have an identical form.[14] For each class with the number of edges q, we assume that the size distribution can be approximated by $F(r) = ar^m$ in the range $r < r_{qp}/2$, where r_{qp} is the normalized grain radius at which the size distribution of class q represents a peak. Defining r_p as the normalized grain radius at which the entire size distribution of all classes represents a peak, we obtain a relationship of $r_{qp}/r_p \approx \bar{r}_q/\bar{r}$ in a steady state, where $\bar{r}_q$ and $\bar{r}$ are the mean values of r_q and r, respectively. Since the ratio $r_p/\bar{r}$ is a constant close to 1 and $\bar{r}_3$ is the smallest value for all classes, we can roughly estimate the applicable range to be $r < \bar{r}_3/2$. The ratio $r_p/\bar{r}$ calculated for the Hillert's and Rayleigh functions is 1.13 and 0.80, respectively. According to experimental observations and numerical simulations, the value of $\bar{r}_3$ is in the range $0.2 \sim 0.4$.[8,10,11,14] This indicates that the applicable range of the function $F(r) = ar^m$ is about $r < 0.1$. For reference, when the Hillert's and Rayleigh functions are approximated by $3\gamma^2 r/4$ and $3\gamma^2 r$ around $r = 0$, as in Section 4.1, the error at $r = 0.1$ is 9.2% and 1.2%, respectively.

4.4 Experiments

The size distribution is known to vary depending on the measuring dimension.[24] Whereas Okazaki and Conrad[15] reported exceptional data for Ti, the distributions of the linear intercept length, the sectional grain area and the grain volume are generally different to each other. Among them, the distribution of the grain volume would be most meaningful, so that the experimental comparison of eq. (10) is preferable for the distribution of the volume-equivalent radius. Most size distributions measured in three dimensions,[15,22–24] however, are not suitable for the present comparison. For example, in the distribution measured by Okazaki and Conrad[15] for Ti, the minimum value of r is about 0.5, and in the distribution by Takayama *et al.*[23] for Al, the minimum value of R is about 180 μm. Since the present analysis concerns the size distribution around $r = 0$, these experimental distributions are not available owing to the lack of data for small grains.

We accordingly compare the present analysis with the distribution of the area-equivalent radius on the sectional surface of 3D polycrystalline materials. The observed distributions of the area-equivalent radius in actual materials show good consistence with the present analysis. For MgO, the size distribution obtained by Aboav and Langdon[27] may be rewritten in a normalized form as[21]

$$F(r) = 0.936 \exp[-9.2524(\sqrt{r} - 0.91398)^2]. \quad (21)$$

The grain growth exponent obtained by Gordon *et al.*[28] is 3, which corresponds to $m = 2$ in eq. (10). As shown in Fig. 3,

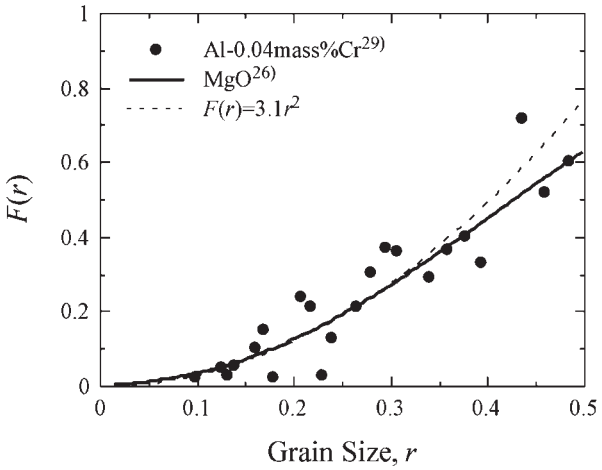

Fig. 3 Experimental size distributions of grains for MgO and Al-0.04 mass%Cr.

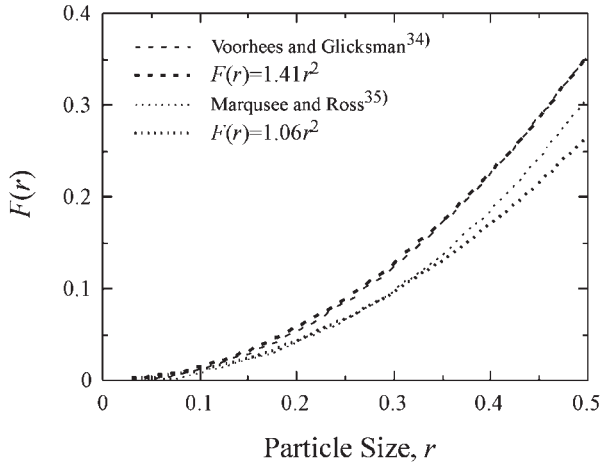

Fig. 4 Theoretical size distributions of small particles for Ostwald-ripening. The volume fraction of particles is 0.35.

eq. (21) around $r = 0$ agrees well with $F(r) = 3.1r^2$, namely $m = 2$ for small grain sizes, showing good consistence with eq. (10).

For Al containing 0.04 mass% Cr, the size distribution obtained by Takayama *et al.*[29] is shown in Fig. 3, where size distributions obtained under four different annealing conditions are superposed. The size distribution of small grains is nearly consistent with that for MgO, and fitted well by $F(r) = 3.1r^2$ ($m = 2$). On the grain growth exponent, $n = 3$ has been reported for pure Al,[30,31] and we consider that the value would not be influenced so much by the addition of 0.04 mass% Cr. Although $n = 4.3$ was obtained by curve fitting for this material,[29] re-analysis of the data shows that the growth behavior can also be explained by $n = 3$. Thus, the experimental distributions of the area-equivalent radius are consistent with the present analysis.

Since the distributions of the area- and the volume-equivalent radii are generally different to each other, the experimental consistence on the sectional surface does not mean the validity of eq. (10) in three dimensions. As noted before, the experimental validity of eq. (10) should be verified from a comparison with the distribution of the volume-equivalent radius. The consistence shown in Fig. 3 may indicate, however, that the characteristics of the size distribution around $r = 0$ are similar between the sectional surface and the 3D space for actual polycrystalline materials, providing that eq. (10) is correct. If so, the size distribution measured on the sectional surface can directly be related to the grain growth kinetics by using eq. (10),

5. Application to the Case of Ostwald-ripening

The present analysis has been conducted under the following conditions: (a) the total volume is conserved, (b) the growth kinetics is represented by eq. (1), (c) the size distribution of grains around $r = 0$ is represented as ar^m, and (d) there exists the grain radius R_h below which grains with 4-faces disappear during Δt in a steady state. These conditions may also be applied to Ostwald-ripening, where the coarsening of secondary phase particles occurs by the annihilation of small particles through diffusion. The only difference is that the value of β is 1 in eq. (2), because all secondary particles are separated and have an identical shape in the particle-coarsening.

For Ostwald-ripening, theoretical models predicted various kinds of particle-size distributions for a steady state. Except for the early predictions by Lifshitz and Slyozov[32] and Wagner,[33] however, the distribution functions are similar to each other in recent models.[34–36] In particular, the size distributions for small particles have a similar form, and hence the difference between the models is quite small. For Ostwald-ripening, the predicted size distributions for small particles can be approximated by $F(r) = ar^2$, as illustrated in Fig. 4. The approximation of ar^2 indicates a growth exponent (n) of 3 in eq. (1), which is just the theoretical n-value for Ostwald-ripening. The r^2-dependency of the size distribution for small particles was also predicted in eq. (16) by the mean field analysis of Coughlan and Fortes.[18] Thus, we conclude that the present analysis is also applicable to the particle coarsening by Ostwald-ripening.

6. Conclusion

We analyzed the theoretical relationship between the kinetics of normal grain growth and the size distribution of small grains. The analysis reveals that the grain growth exponent n is equal to $m + 1$, when the distribution of the normalized grain size r is proportional to r^m around $r = 0$. The physical basis of the size distribution r^{n-1} around $r = 0$ has been derived from the mean field model for particle growth. Although an infinite number of size distributions can exist in a steady state, the relationship $n = m + 1$ provides the criteria which should be satisfied. Comparison of the relationship with other theoretical and empirical models shows that the Hillert's and Rayleigh distribution functions for small grains are consistent well with the present analysis, while the log-normal function does not represent the size distribution in the steady normal grain growth with $n = 2$. The validity of the present analysis is also supported by the agreement with numerical simulations. Consistence is observed between the present analysis and the size distributions experimentally measured on the sectional surface of actual

polycrystals. We also showed that the present relationship, $n = m + 1$, holds for particle coarsening by Ostwald-ripening.

Acknowledgements

The authors would like to thank Prof. Y. Takayama for his helpful data and comments.

REFERENCES

1) M. Hillert: Acta Metall. **13** (1965), 227-238.
2) N. P. Louat: Acta Metall. **22** (1974), 721-724.
3) K. Lucke, I. Heckelmann and G. Abbruzzese: Acta Metall. Mater. **40** (1992) 533-542.
4) C. S. Pande: Acta Metall. **35** (1987), 2671-2678.
5) M. P. Anderson, G. S. Grest and D. J. Srolovitz: Philos. Mag. **B59** (1989) 293-329.
6) K. Fuchizaki, T. Kusaba and K. Kawasaki: Philos. Mag. **B71** (1995) 333-357.
7) B. Radhakrishnan and T. Zacharia: Metall. Mater. Trans. **26A** (1995) 167-180.
8) S. P. Gill and A. C. F. Cocks: Acta Mater. **44** (1996) 4777-4789.
9) K. Marthinsen, O. Hunderi and N. Ryum: Acta Mater. **44** (1996) 1681-1689.
10) D. Weygand, Y. Brechet and J. Lepinoux: Philos. Mag. **B78** (1998) 329-352.
11) B.-N. Kim: Mater. Sci. Eng. **A283** (2000) 164-171.
12) F. Wakai, N. Enomoto and H. Ogawa: Acta Mater. **48** (2000) 1297-1311.
13) P. Feltham: Acta Metall. **5** (1957) 97-105.
14) S. K. Kurtz and F. M. A. Carpay: J. Appl. Phys. **51** (1980) 5745-5754.
15) K. Okazaki and H. Conrad: Trans. JIM **13** (1972) 198-204.
16) W. W. Mullins: J. Appl. Phys. **27** (1956) 900-904.
17) W. W. Mullins: Acta Metall. **37** (1989) 2979-2984.
18) S. D. Coughlan and M. A. Fortes: Scripta Metall. Mater. **28** (1993) 1471-1476.
19) P. R. Rios: Scr. Mater. **40** (1999) 665-668.
20) L. C. Brown: Acta Metall. **37** (1989) 71-77.
21) C. S. Pande, R. A. Masumura and S. P. Marsh: Acta Mater. **45** (1997) 4361-4366.
22) F. N. Rhines and B. R. Patterson: Metall. Trans. **13A** (1982) 985-993.
23) Y. Takayama, T. Tozawa, H. Kato and H. Shirai: J. Japan Inst. Light Metals **40** (1990) 612-618.
24) F. Schückher: *Quantitative Microscopy*, ed. by R. T. DeHoff and F. N. Rhines, (McGraw-Hill, New York, 1968) pp. 201-265.
25) Y. Takayama, N. Furushiro, T. Tozawa, H. Kato and S. Hori: Mater. Trans., JIM **32** (1991) 214-221.
26) H. V. Atkinson: Acta Metall. **36** (1988) 469-491.
27) D. A. Aboav and T. G. Langdon: Metallography **6** (1973) 9-15.
28) R. S. Gordon, D. D. Marchant and G. W. Hollenberg: J. Am. Ceram. Soc. **53** (1970) 399-406.
29) Y. Takayama, T. Tozawa, H. Kato, S. Kato, N. Furushiro and S. Hori: J. Japan Inst. Metals **52** (1988) 465-471.
30) P. Gordon and T. A. El-Bassyouni: Trans. TMS-AIME **233** (1965) 391-397.
31) F. N. Rhines and K. R. Craig: Metall. Trans. **5** (1974) 413-425.
32) I. M. Lifshitz and V. V. Slyozov: J. Phys. Chem. Solids **19** (1961) 35-50.
33) C. Wagner: Z. Elektrochem **65** (1961) 581-591.
34) P. W. Voorhees and M. E. Glicksman: Acta Metall. **32** (1984) 2013-2030.
35) J. A. Marqusee and J. Ross: J. Chem. Phys. **80** (1984) 536-543.
36) Y. Enomoto, K. Kawasaki and M. Tokuyama: Acta Metall. **35** (1987) 907-913.